Unsteady convective diffusion with Interphase mass transfer in Bingham fluid through porous medium

Suchita T.S [1], S Senthamilselvi[1] and R. VijayaKumar[2]

[1]*Department of Mathematics,Vels Institute of Science, Technology & Advanced Studies,Tamil Nadu, India.*
[2]*Mathematics Section,FEAT,Annamalai University, Annamalainagar-608002,India.Department of Mathematics, Periyar Government Arts College, Cuddalore,TamilNadu – 607 001, India. Email: rathirath_viji@yahoo.co.in*

Corresponding author Email: msselvi2305@gmail.com

KEYWORDS

Bingham fluid, Magnetic field, First-order reactions, Generalized dispersion model.

ABSTRACT

The current study goal is to disperse a solute at the parallel channel boundary walls as it undergoes an irreversible first-order chemical reaction. The rheological parameter that occurs from suspension in the fluid affects the convection coefficient and dispersion coefficient. The interphase mass transfer is the main cause of the exchange coefficient, which is unaffected by the solvent fluid velocity. The convection and dispersion coefficients are also affected by the wall-catalyzed process. The transfer of drugs or nutrients in plasma during blood flow through porous media can be understood by studying solute dispersion. An essential part of circulatory flow is exceed absorption. The results show that wall absorption has a significant impact on transport coefficients.

Nomenclature

u_f^*	component of velocity $(\mathrm{m/s})$
p^*	pressure
μ	viscosity of the fluid
B_0	applied magnetic field
σ_0	electrical conductivity,
t	time,
D	molecular diffusivity
k	permeability of the porous medium
u_p^*	Darcy velocity,
α	slip parameter,
$C_0^{'}$	reference concentration and
Ks	reaction rate constant catalyzed by the walls.
τ_{xy}	shear stress
μ_0	plastic dynamic viscosity
τ_0	yield stress

1. Introduction

In physiological situations where a first-order chemical reaction takes place at the tube wall, interphase mass transfer can be used. Transporting oxygen and nutrients to tissue cells and extracting metabolic waste products from tissue cells are two examples of such circumstances. It also occurs in the pulmonary capillaries, where the blood absorbs oxygen and carbon dioxide is expelled. Many studies on the fluid dynamics of biological fluids under the influence of magnetic fields have been conducted in the past ten years. The lack of biocompatibility of smooth (rough) surfaces in metal-implanted or extracorporeal artificial organs results in a variety of blood injury types. It is dangerous since they create stress that results in force. Eventually, this force affects the red blood cells, or erythrocytes, causing haemolysis, or the loss of haemoglobin. Several authors focused on dispersion to understand the transport of nutrients in blood and different artificial devices (Middleman (1972), Lightfoot (1974), Cooney (1976), Jayaraman et al., (1981)). The effective dispersion coefficient was examined in relation to the average flow speed, the tube radius, and the molecular diffusion coefficient by Taylor (1953, 1954), who investigated the dispersion process in Newtonian flow. Sankarasubramanian and Gill (1973) explored the dispersion of a non-uniform initial distribution in time-variable isothermal laminar flow in a tube with a first-order rate process near the tube wall. Through a precise process, they investigated miscible dispersion in laminar flow in a tube with interfacial transport caused by an irreversible first-order reaction at the tube wall. The exchange coefficients are a novel idea, and a generic formula demonstrating their time-dependent character is constructed. Finding the average concentration distribution in terms of tabular functions is made possible by the exchange coefficient, which represents the interphase process. Only the scenario of dispersion in a fully established steady flow was included in the analysis.

Siddheshwar et al. (2000) have studied the problem of plane-Poiseuille flow of a power law fluid with interphase mass transfer. Indira et al. (1996) looked on the precise study of miscible solute dispersion with interphase mass transfer in a couple stress fluid flow. Unsteady convective diffusion with interphase mass transfer in a couple stress fluid surrounded by porous beds has been studied by Manjula (2008). Using the generalised dispersion model of Sankarasubramanian and Gill (1970), Nirmala P. Ratchagar and Vijaya Kumar (2015) examined the impact of couple stress and magnetic field on unstable convective diffusion with interphase mass transfer. In the simplest scenario, they take into account a first order chemical reaction at the walls during an exact analysis of unsteady convection in couple stress fluid flows. Reaction at the walls is of practical interest. The exact analysis of miscible solute dispersion with interphase mass transfer in a couple stress poorly conducting fluid surround by porous beds was examined by Rudraiah et al. (2016). The exchange coefficient, convective coefficient, and dispersion coefficient are highlighted by the utilization the generalised dispersion model of Sankarasubramanian and Gill's (1973). The porosity parameter and couple stress parameter resulting from suspension in the fluid only affect the final two coefficients. The interphase mass transfer is the primary cause of the exchange coefficient, which is unaffected by the solvent fluid velocity. The convection and dispersion coefficients are also impacted by the interphase mass transfer.

Siti Nurul Aifa Mohd Zainul Abidin (2024) explored the Herschel-Bulkley (H-B) fluid model, a non-Newtonian mathematical model of blood flow in a catheterised stenosed artery. Additionally, the wall absorption effect is taken into account in this inquiry. The convective-diffusion equation that describes the dispersion process determines the solute movement. Three effective transport coefficients exchange, convection, and diffusion are obtained by solving the transport equation using an accurate technique known as the Generalised Dispersion Model (GDM). The goal of this work has been to examine the flow properties of a Bingham plastic fluid through a porous material when both an electric and magnetic field are present. In order to emphasise the dispersion coefficient and mean concentration, the generalised dispersion model of Sankarasubramanian and Gill (1970) has been applied. Convection coefficient and dispersion coefficient are affected by the rheological parameter , magnetic field, electric number and porous parameter arising due to suspension in the fluid. The exchange coefficient arises mainly due to the interphase mass transfer, and it is independent of the solvent fluid velocity. The convection and dispersion coefficients are also affected by the interphase mass transfer. Finally the outcome of non-dimensional parameter is deliberated by graphs.

2. Mathematical Formulation

The constitutive equation for blood, expressed as Bingham fluid, is as follows, according to Misra and Adhikary (2017)

$$\tau_{xy} = -\mu_0 \frac{\partial u_f^*}{\partial y} \pm \tau_0 \qquad if \qquad \left|\tau_{xy}\right| > \tau_0 \tag{1}$$

$$\frac{\partial u_f^*}{\partial y} = 0 \qquad if \qquad \left|\tau_{xy}\right| < \tau_0 \tag{2}$$

In the channel, equations (1) and (2) depict the two stages of blood flow. The flat velocity profile in the central core region creates the plug flow region. Shear stress in this plug flow zone is less than yield stress τ_0.

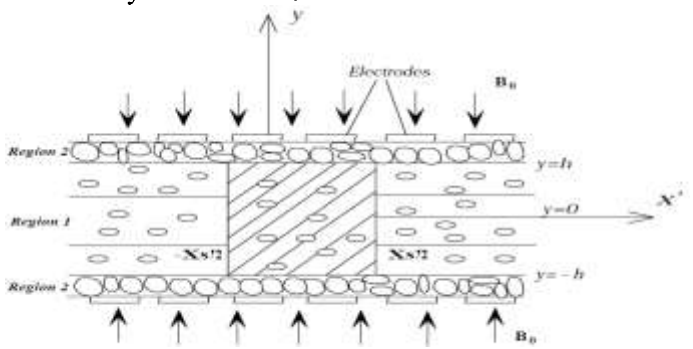

Figure 1: Physical problem

The governing equations and associated boundary conditions are derived under the following presumptions:

An electric field and a uniform magnetic field B_0 are supplied to the blood flow in the y-direction. In a channel enclosed by porous beds, the solute diffuses over the porous medium in a fully formed flow. For concentration C, which depends on coordinates x' and y and time (t), a slug is added. The mass balance equation concerning the solute concentration C with heterogeneous chemical reaction. Under the aforementioned presumption, the following governing equations apply to the incompressible flow of a non-Newtonian fluid in cartesian coordinates:

Region 1:

$$\frac{\partial u_f^*}{\partial x'} = 0 \tag{3}$$

$$-\frac{\partial p'}{\partial x'} + \mu \frac{\partial \tau_{xy}}{\partial y} - \frac{\mu}{k} u_f^* - B_0^2 \sigma_0 u_f^* + \rho_e E_x = 0 \tag{4}$$

$$-\frac{\partial p'}{\partial y} + \rho_e E_y = 0 \tag{5}$$

The concentration C satisfying the convective diffusion equation gives

$$\frac{\partial C}{\partial t} + u_f^* \frac{\partial C}{\partial x'} = D\left(\frac{\partial^2 C}{\partial x'^2} + \frac{\partial^2 C}{\partial y^2}\right) \tag{6}$$

Region 2:

$$\frac{\partial u_p^*}{\partial x} = 0 \tag{7}$$

$$-\frac{\partial p'}{\partial x'} - \frac{\mu}{k} u_p^* + -B_0^2 \sigma_0 u_p^* + \rho_e E_x + \alpha_0 = 0 \tag{8}$$

$$-\frac{\partial p'}{\partial y} + \rho_e E_y = 0 \tag{9}$$

Boundary conditions for velocity and concentration are

$$\frac{\partial u_f^*}{\partial y} = -\frac{\alpha}{\sqrt{k}} (u_f^* - u_p^*) \qquad at \qquad y = h \tag{10}$$

$$\frac{\partial u_f^*}{\partial y} = \frac{\alpha}{\sqrt{k}} (u_f^* - u_p^*) \qquad at \qquad y = -h \tag{11}$$

The symmetric conditions,

$$\frac{\partial u_f^*}{\partial y} = 0 \qquad at \qquad y = 0 \tag{12}$$

$$u_f^* = u_{pf}^* \qquad at \qquad y = y_c \tag{13}$$

$$C' = C_0' \psi_1(x') Y_1(y) \qquad at \qquad t = 0 \tag{14}$$

$$\left.\begin{array}{l} -D\dfrac{\partial C'}{\partial y}(t, x', h) = K_s C' \\ D\dfrac{\partial C'}{\partial y}(t, x', -h) = K_s C' \end{array}\right\} \tag{15}$$

As the amount of solute in the system is finite,

$$C'(t, \infty, y) = \frac{\partial C'}{\partial x'}(t, \infty, y) = 0 \tag{16}$$

Beavers and Joseph's (1967) slip condition at the lower and upper permeable surfaces is represented by equations (10) and (11).
Introducing the non-dimensional quantities

$$U_f = \frac{u_f^*}{u'}, U_p = \frac{u_p^*}{u'}, \eta = \frac{y}{h}, X' = \frac{x'}{hPe}, X'_s = \frac{x'_s}{hPe}, Pe = \frac{u'h}{D}, p* = \frac{p}{\rho u'^2}, \tau = \frac{Dt}{h^2}, \theta = \frac{C'}{C_0},$$

$$\beta = \frac{k_s h}{D}, \rho_e = \frac{\hat{\rho}_0 h^2}{\in_0 V}, E'_x = \frac{E_x h}{V}$$

In non-dimensional form, equations (3) to (9) are
Region 1:

$$\frac{d^4 U_f}{\partial \eta^4} - M^2 U_f = s_2 + We\, s_1 (1 - \alpha_c \eta) \tag{17}$$

$$\frac{\partial \theta}{\partial \tau} + U_f \frac{\partial \theta}{\partial X'} = \frac{1}{Pe^2}\left(\frac{\partial^2 \theta}{\partial X'^2} + \frac{\partial^2 \theta}{\partial \eta^2}\right) \tag{18}$$

we define the axial coordinate moving with the average velocity of flow as $x = x' - tu'$ which is in dimensionless form $X = X' - \tau$,.
Then equation (13) becomes

$$\frac{\partial \theta}{\partial \tau} + U_f' \frac{\partial \theta}{\partial X} = \frac{1}{Pe^2}\left(\frac{\partial^2 \theta}{\partial X^2} + \frac{\partial^2 \theta}{\partial \eta^2}\right) \tag{19}$$

where, $U_f' = \dfrac{U_f - \bar{U}_f}{\bar{U}_f}$

Region 2:

$$U_p = -\frac{\left[\dfrac{\text{Re}}{Pe} + We\, s_1 (1 - \alpha_c \eta)\right]}{\sigma^2 + M^2} \tag{20}$$

The dimensionless form of the initial and boundary conditions (10) to (16)

$$\frac{\partial U_f}{\partial \eta} = -\alpha\sigma(U_f - U_p) \qquad at \qquad \eta = 1 \tag{21}$$

$$\frac{\partial U_f}{\partial \eta} = \alpha\sigma(U_f - U_p) \qquad at \qquad \eta = -1 \tag{22}$$

$$\frac{\partial U_f}{\partial \eta} = 0 \qquad at \qquad \eta = 0 \tag{23}$$

$$U_f = U_{pf} \qquad at \qquad \eta = \eta_c \tag{24}$$

$$\theta = \psi(X) Y(\eta) \qquad at \qquad \tau = 0 \tag{25}$$

$$\left.\begin{array}{l} \dfrac{\partial \theta}{\partial \eta}(\tau, X, 1) = -\beta\theta \\ \dfrac{\partial \theta}{\partial \eta}(\tau, X, -1) = \beta\theta \end{array}\right\} \tag{26}$$

$$\theta(\tau,\infty,\eta)=\frac{\partial\theta}{\partial X}(\tau,\infty,\eta)=0 \tag{27}$$

where $M^2=\frac{B_0^2\sigma_0 h^2}{\mu}$ is the square of the Hartmann number, $We=\frac{\varepsilon_0 V^2}{\mu_0}$ is the electric numbers $P=-\frac{\mathrm{Re}}{Pe}\frac{\partial p}{\partial X'}, \mathrm{Re}=\frac{\rho u' h}{\mu}$ is the Reynolds number, $Pe=\frac{u' h}{D}$ is the Peclet number, $\sigma=\frac{h}{\sqrt{k}}$ is the porous parameter, K_s is the reaction rate constant catalyzed by the walls.

3. Method of solution

By solving equation (17) and satisfying the boundary conditions (21) to (24). The blood velocity is obtained as

$$U_f=\begin{cases} A_1e^{M\eta_c}+A_2e^{-M\eta_c}-\frac{1}{M^2}We \;\; s_1(1-\alpha_c\eta_c), \; if \;\; 0<\eta\le\eta_c \\ A_1e^{M\eta}+A_2e^{-M\eta}-\frac{1}{M^2}We \;\; s_1(1-\alpha_c\eta), \; if \;\; \eta_c<\eta\le 1 \end{cases} \tag{28}$$

where A_1, A_2, and s_1 are constants given in Appendix 1.

The axial velocity components that have been normalised are

$$U_f^{'}=\frac{U_f-\bar{U}_f}{\bar{U}_f} \tag{29}$$

where

$$\bar{U}_f=\int_0^1 U_f(\eta)d\eta=\eta_C\left(A_1e^{M\eta_c}+A_2e^{-M\eta_c}-\frac{1}{M^2}We \;\; s_1(1-\alpha_c\eta_c)\right)+\frac{1}{2M}\{\left(A_2(2e^{-M}-2e^{-M\eta_c})\right)-2A_1(2e^M-e^{M\eta_c})$$
$$+s_1We(-1+\eta_c)(-2+\alpha_c+\alpha_c\eta_c)\} \tag{30}$$

The generalised dispersion model of Gill and Sankarasubramanian (1970), which is expressed as a series expansion in the form of

$$\theta(\tau,X,\eta)=\theta_m(\tau,X)+f_1(\tau,\eta)\frac{\partial\theta_m}{\partial X}+f_2(\tau,\eta)\frac{\partial^2\theta_m}{\partial X^2}+... \tag{31}$$

where, θ_m is the dimensionless cross sectional average concentration, given by

$$\theta(\tau,X)=\int_0^1\theta(\tau,X,\eta)d\eta \tag{32}$$

Integrating equation (19) with respect to η in (0,1) and using the equation (31) and (32), we get

$$\frac{\partial\theta_m}{\partial\tau}=\frac{1}{Pe^2}\frac{\partial^2\theta}{\partial X^2}-\frac{\partial}{\partial X}\int_0^1 U_f^{'}\left(\theta_m(\tau,X)+f_1(\tau,\eta)\frac{\partial\theta_m}{\partial X}+f_2(\tau,\eta)\frac{\partial^2\theta_m}{\partial X^2}+...\right)d\eta \tag{33}$$

In this model we write

$$\frac{\partial\theta_m}{\partial\tau}=\sum_{k=0}^{\infty}K_k(\tau)\frac{\partial^k\theta}{\partial X^k} \tag{34}$$

where the dispersion coefficient, $K_k(\tau)$ Substituting the Equation (34) in (33) we obtain

$$K_0\theta_m+K_1(\tau)\frac{\partial\theta}{\partial X}+K_2(\tau)\frac{\partial^2\theta}{\partial X^2}+K_3(\tau)\frac{\partial^3\theta}{\partial X^3}+......=\frac{1}{Pe^2}\frac{\partial^2\theta}{\partial X^2}+\left[\frac{\partial}{\partial\eta}(f_0\theta_m+f_1\frac{\partial\theta_m}{\partial X})\right]_0^1$$
$$-\frac{\partial}{\partial X}\int_0^1 U_f'\left(f_0(\tau,\eta)\theta_m(\tau,X)+f_1(\tau,\eta)\frac{\partial\theta_m}{\partial X}+f_2(\tau,\eta)\frac{\partial^2\theta_m}{\partial X^2}+...\right)d\eta$$

Equating the coefficient $\frac{\partial\theta_m}{\partial X},\frac{\partial^2\theta_m}{\partial X^2},...,$.we get,

$$K_i(\tau)=\frac{\delta_{ij}}{Pe^2}+\frac{1}{2}\frac{\partial f_i}{\partial X}(\tau,1)-\int_0^1 U_f'\,f_{i-1}(\tau,\eta)\,d\eta \qquad (i=1,2,3,....\;) \tag{35}$$

where $f_{-1}=0$

Equation (35) can be truncated after the term involving K_2 without causing serious error, because $K_3, K_4,$, etc. become negligibly small compared to K_2.

The resulting model for the mean concentration is

$$\frac{\partial \theta_m}{\partial \tau} = K_0\theta_m + K_1(\tau)\frac{\partial \theta}{\partial X} + K_2(\tau)\frac{\partial^2 \theta}{\partial X^2} \qquad (36)$$

Substituting (31) in (19) and using the generalized dispersion model of Gill and Sankarasubramanian(1973) in the resulting equation, we get the equation for f_k from the differential equations of the form

$$\frac{\partial f_k}{\partial \tau} = \frac{\partial^2 f_k}{\partial \eta^2} - U_f{}' f_{k-1} + \frac{1}{Pe^2} f_{k-2} = \sum_{i=0}^{k} K_i f_{k-i} \qquad (k = 0,1,2,...) \qquad (37)$$

where, $f_{-1} = f_{-2} = 0$

Since θ_m is chosen to satisfy the initial and boundary conditions on θ from equations (25) to (26) conditions on the f_k function becomes

$$f_k = finite \quad at \quad \tau = 0 \qquad (38)$$

$$\frac{\partial}{\partial \eta} f_k(\tau,1) = -\beta f_k \qquad (39)$$

$$\frac{\partial}{\partial \eta} f_k(\tau,0) = 0 \qquad (40)$$

Also, from equation (32) we have

$$\int_0^1 f_k(\tau,\eta)d\eta = \delta_{k0}, (k = 0,1,2) \qquad (41)$$

Substituting k = 0 in equation (37) we get the differential equation for f_0 as

$$\frac{\partial f_0}{\partial \tau} = \frac{\partial^2 f_0}{\partial \eta^2} - f_0 K_0 \qquad (42)$$

For i = 0 in (30) we have

$$K_0(\tau) = \left[\frac{\partial f_0}{\partial \eta}\right]_0^1 - f_0 K_0 \qquad (43)$$

These two equations (42) and (43) must be solved simultaneously, with an initial condition for using (32) that requires entering that equation to obtain

$$\theta_m(0,X) = \int_0^1 \theta_m(0,X,\eta)d\eta \qquad (44)$$

Substituting $\tau = 0$ in (31) and setting $f_k(\eta) = 0\,(k = 1,2,3)$ gives the initial condition for f_0 as

$$f_0(0,\eta) = \frac{\theta(0,X,\eta)}{\theta_m(0,X)} \qquad (45)$$

Substituting equation (39) and (40) into equation (45),
we get

$$f_0(0,\eta) = \frac{\psi(\eta)}{\frac{1}{2}\int_{-1}^{1}\psi(\eta)d\eta} \qquad (46)$$

The solution of the reaction diffusion equation (42) with these conditions are formulated as

$$f_0(\tau,\eta) = g_0(\tau,\eta)\exp\left[-\int_0^1 K_{0I}(\eta)d\eta\right] \qquad (47)$$

from which it follows that $g_0(\tau,\eta)$ has to satisfy

$$\frac{\partial g_0}{\partial \tau} = \frac{\partial^2 g_0}{\partial \eta^2} \qquad (48)$$

with conditions

$$f_0 = g_0 = \frac{\psi(\eta)}{\frac{1}{2}\int_{-1}^{1}\psi(\eta)d\eta} \quad at \quad \tau = 0 \tag{49}$$

$$g_0 = finite \quad at \quad \eta = 0 \tag{50}$$

$$\frac{\partial g_0}{\partial \eta} = -\beta g_0 \quad at \quad \eta = 1 \tag{51}$$

The solution of (48) subject to conditions (49) to (51) is

$$g_0(\tau,\eta) = \sum_{n=0}^{\infty} A_n e^{-\mu_n^2 \tau} Cos(\mu_n \eta) \tag{52}$$

where $\mu_n 's$ are the roots of

$$\mu_n \tan \mu_n = \beta, \quad n = 0,1,2,... \tag{53}$$

andAn 's are given by

$$A_n = \frac{\int_0^1 \psi(\eta)\cos\mu_n\eta\, d\eta}{\left(1 + \frac{\sin 2\mu_n}{2\mu_n}\right)\int_0^1 \psi(\eta)d\eta} \tag{54}$$

From(47), it follows that

$$f_0(\tau,\eta) = \frac{2g_0(\tau,\eta)}{\int_0^1 g_0(\tau,\eta)d\eta} = \frac{\sum_{n=0}^{\infty} A_n e^{-\mu_n^2\tau} Cos(\mu_n\eta)}{\sum_{n=0}^{\infty} \frac{A_n}{\mu_n} e^{-\mu_n^2\tau} Sin\,\mu_n} \tag{55}$$

MATHEMATICA 12.0 is used to obtain the first ten roots of the transcendental equation (53), which are listed in Table 1. In the expansions of and, these 10 roots ensure the series will converge. With that, we obtain from (48) in the form

$$K_0(\infty) = \frac{\sum_{n=0}^{\infty} A_n \mu_n e^{-\mu_n^2\tau} Sin(\mu_n\eta)}{\sum_{n=0}^{\infty} \frac{A_n}{\mu_n} e^{-\mu_n^2\tau} Sin\,\mu_n} \tag{56}$$

Here $K_0(\tau)$ is independent of velocity distribution.

As $\tau \to \infty$, we get the asymptotic solution for K_0 from (56) as

$$K_0(\infty) = -\mu_0^2 \tag{57}$$

where μ_0 is the first root of the equation (53). Physically, this represents first order chemical reaction coefficient to obtain $K_0(\infty)$. We get $K_1(\infty)$, from (35) (with i = 1) knowing $f_0(\infty,\eta)$ and $f_1(\infty,\eta)$. Likewise, $K_2(\infty), K_3(\infty),....,$
require the knowledge of $K_0, K_1, f_0, f_{1,}$ and f_2. Equation (55) in the limit $\tau \to \infty,$ reduces to

$$f_0(\infty,\eta) = \frac{\mu_0}{Sin\,\mu_0} Cos(\mu_0) \tag{58}$$

Then we find $f_1\ K_1,\ f_2$ *and* K_2. For asymptotically long times, i.e.,$\tau \to \infty$, equation (35) and (37) give $K_i 's$ *and* $f_k 's$ as

$$K_i(\tau) = \frac{\delta_{ij}}{Pe^2} - \beta f_i(\infty,1) - \int_0^1 U'\, f_{i-1}(\infty,\eta)\,d\eta \qquad (i = 1,2,3,....\ ) \tag{59}$$

$$\frac{\partial^2 f_k}{\partial \eta^2} + \mu_0^2 f_k = (U'+K_1) f_{k-1} - \left(\frac{1}{Pe^2} - K_{2I}\right) f_{k-2}, \quad (k = 1,2,...) \tag{60}$$

The $f_k 's$ must satisfy the conditions (32) and this permits the eigen function expansion in the form of

$$f_k(\infty,\eta) = \sum_{j=0}^{9} B_{j,k} Cos(\mu_j \eta),\ k = 1,23,.. \tag{61}$$

Substituting (61) in (60) and multiplying the resulting equation by $\cos(\mu_j\eta)$ and integrating with respect to η from 0 to 1, gives

$$B_{j,k}\,Cos(\mu_j\eta)=\frac{1}{\mu_j^2-\mu_0^2}\left[\frac{1}{Pe^2}\sum_{j=0}^{9}B_{j,k-2}Cos(\mu_j\eta)-U_f{}'\sum_{j=0}^{9}B_{j,k-1}Cos(\mu_j\eta)-\sum_{j=0}^{9}K_{il}B_{j,k-i}Cos(\mu_j\eta)\right]$$

Multiplying by $Cos(\mu_j\eta)$ and integrating with respect to η, we get

$$B_{j,k}=\frac{1}{\mu_j^2-\mu_0^2}\left[\frac{1}{Pe^2}\sum_{j=0}^{9}B_{j,k-2}-U'\sum_{j=0}^{9}B_{j,k-1}-\left(1+\frac{Sin\,\mu_j}{2\mu_j}\right)^{-1}\sum_{j=0}^{9}B_{j,k-i}\,I(j,l)\right]\quad k=(1,2)\qquad(62)$$

Where

$$I(j,l)=\int_0^1 U'Cos(\mu_j\eta)Cos(\mu_l\eta)d\eta=I(l,j)\qquad(63)$$

$$B_{j,-1}=0,B_{j,0}=0\qquad for\quad j=1\quad to\quad 9\qquad(64)$$

The first expansion coefficient $B_{0,k}$ in equation (61) using conditions (38) to (41) can be expressed in terms of $B_{j,k}$ (j = 1 to 9) as, (Using the boundary condition $\int_0^1 f_k(\tau,\eta)d\eta=\delta_{k0}=0$)

$$B_{0,k}=-\left(\frac{\mu_0}{\sin\mu_0}\right)\sum_{j=0}^{9}B_{j,k}\,\frac{Sin\,\mu_j}{2\mu_j}\quad k=(1,2,3,...)\qquad(65)$$

Further, from (57) and (61) we find that

$$B_{0,0}=\frac{\mu_0}{Sin\,\mu_0}\qquad(66)$$

Using (63), (64) and (66) in the resultant equation after substituting i = 1 in (59), we obtain

$$K_1(\infty)=-\frac{I(0,0)}{\left[1+\frac{Sin\,2\mu_0}{2\mu_0}\right]}\qquad(67)$$

Using (62), (63) and (66) in the the outcome equation after substituting i = 2 in (59), we obtain

$$K_2=\frac{1}{Pe^2}-\frac{\sin\mu_0}{\mu_0\left(1+\frac{Sin\,2\mu_0}{2\mu_0}\right)}\sum_{j=0}^{9}B_{j,k-i}\,I_{j,0}\qquad(68)$$

where $B_{j,1}=-\frac{1}{\mu_j^2-\mu_0^2}\left(1+\frac{Sin\,\mu_j}{2\mu_j}\right)^{-1}\frac{\mu_0}{Sin\,\mu_0}I(j,0)$

The mean concentration distribution as a function of and the parameters Pe, and is found using the asymptotic coefficients in (32).This distribution is an approximate representation for short and moderate times and is valid for a long duration. By calculating the cross-sectional average from (25) the initial condition for solving (34) may be obtained. According to Sankar Rao (1995), the solution of (34) with asymptotic coefficients may be expressed as follows: Long-term evaluations of the coefficients have an impact that is independent of the initial concentration distribution.

$$\theta_m(\tau,X)=\frac{1}{2Pe\sqrt{\pi K_2(\infty)\tau}}\exp\left[K_0(\infty)\tau-\frac{\left[X+K_1(\infty)\tau\right]^2}{4K_2(\infty)\tau}\right]\qquad(69)$$

where $\theta_m(\tau,\infty)=0,\ \frac{\partial\theta_m}{\partial X}(\tau,\infty)=0$

4. Results and Discussion

The effects of magnetic field, electric field, and heterogeneous chemical reactions on the dispersion of a solute in a Bingham fluid (blood) as it flows through a porous medium in a rectangular channel enclosed by porous beds are examined. The channel walls act as catalysts for the reaction. Figures 2 to 16 show the graphic representation of the most dominant dispersion coefficient, convection coefficient, and mean concentration for fixed values using MATHEMATICA 12.0. These values are calculated for different values of Hartmann number(M=1,1.1,1.2,1.3), porous parameter $(\sigma=10,60,100,120)$, rheological parameter $(\eta_c=0,0.1,0.2,0.3)$, reaction rate parameter $(\beta=10^{-2},1,10^{2})$ and electric number(We=5, 15,25,35) for fixed values $X_s=0.019, X=0.1, Pe=100, \alpha=0.10$.

Equation (57), which is used to numerically assess the expression for the absorption coefficient $-K_0(\infty)$, is displayed in Figure 2. Although it is unaffected by the Hartmann number, porous parameter, rheological parameter, it is clear that the increases as the wall reaction parameter β grows. Molecular diffusion can provide the reaction at the wall more quickly if the absorption parameter takes huge values. Therefore, compared to tubular flow, there is greater solute absorption at the annulus wall.

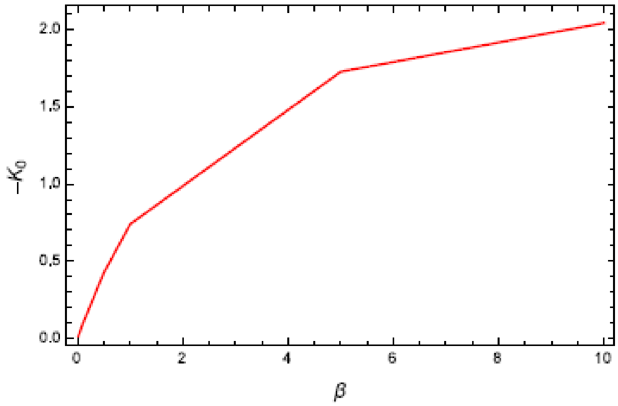

Figure 2: Variation of $-K_0$ versus β

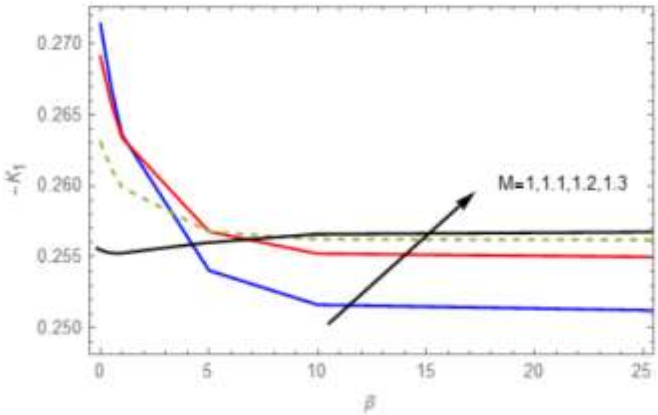

Figure 3: Impact of M on $-K_1$

The variance of the convection and dispersion coefficients diminishes as the range of the wall reaction parameter β grows as seen in Figures 3 to 10. This phenomenon is attributed to the synergistic effect of magnetic field strength and wall reaction parameter, enhancing the decline in convection and dispersion coefficients (Singh, J., and Kumar, V. (2020)). Figures 3 to 6 display the convection coefficient expression for different values of the Hartmann number, electric number, rheological parameter, and porous parameter with wall response parameter. These expressions are numerically analysed using equation (67). It is observed that the convection coefficient decreases with increases in the Hartmann number, electric number, rheological parameter, and porous parameter. The increase in Hartmann number, electric number, rheological parameter, and porous parameter enhances the convection coefficient in blood flow due to the augmented Lorentz force, electrical body force, and porous medium resistance, which intensify the flow velocity and mixing, thereby increasing dispersion(Tripathi and Kumar(2020))

Equation (68) is used to numerically assess the expression for the dispersion coefficient, which is displayed in Figures 7 to 11 for varying Hartmann number, electric number, rheological parameter, and porous parameter values with wall reaction parameter values. As η_c grows in the flow of a Bingham fluid, the area of the plug flow zone also increases, which should naturally tend to raise the dispersion coefficient in Figure 10. Nevertheless, the velocity gradient in the shear flow zone $\eta > \eta_c$ changes as η_c increases. Additionally, the exact value of $K_2(\tau) - Pe^{-2}$ depends on two conflicting effects: an increase in $K_2(\tau) - Pe^{-2}$ owing to a shift in the velocity gradient in the shear flow zone and a increase in $K_2(\tau) - Pe^{-2}$ due to an increase in the plug flow region. The former impact outweighs the latter for all η due to the two-dimensional structure of the flow in a channel, and we see a monotonic drop in $K_2(\tau) - Pe^{-2}$ as η_c increases. When $\eta_c = 0$, (68) gives Annapurna and Gupta(1979). Plotting the dispersion coefficient versus reaction rate parameter values is shown in Figures 7 to 9. It is found that when the Hartmann number, electric number and porous parameter decreases, the dispersion coefficient rises. As a result, the laminar flow is maintained.

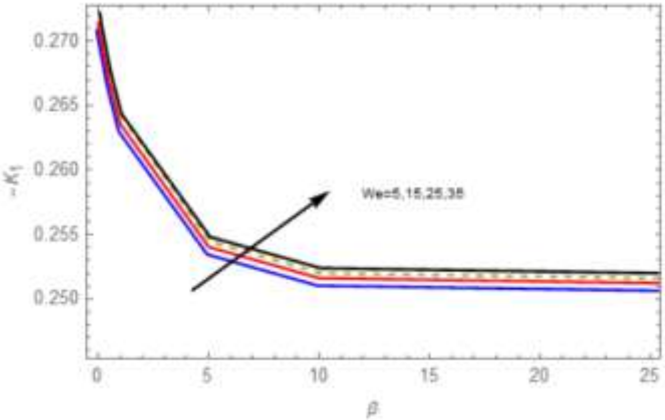

Figure 4: Impact of We on $-K_1$

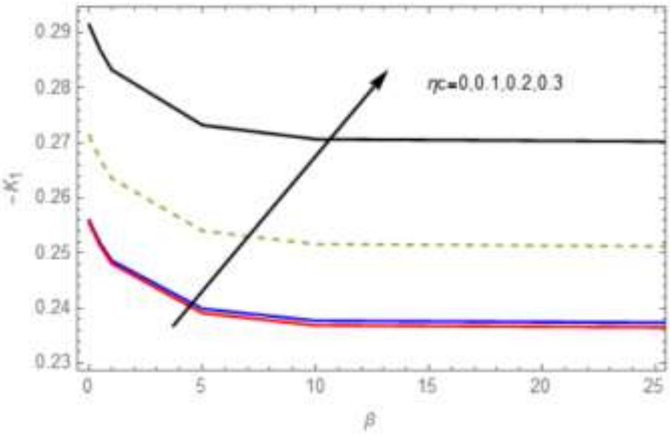

Figure 5: Impact of η_c on $-K_1$

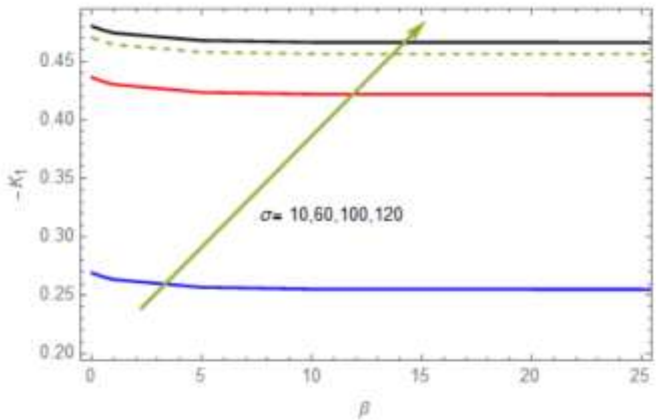

Figure 6: Impact of σ on $-K_1$

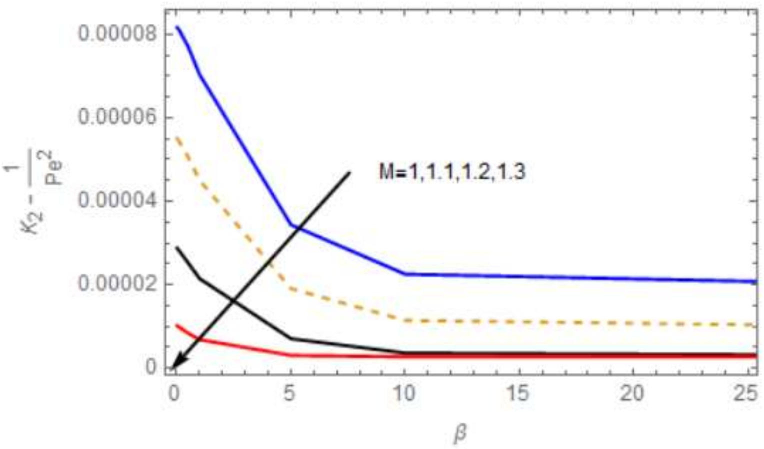

Figure 7: Impact of M on $K_2(\tau) - Pe^{-2}$

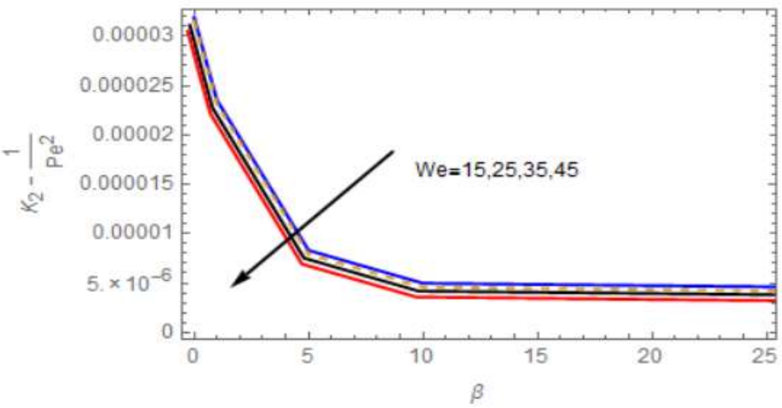

Figure 8: Impact of We on $K_2(\tau) - Pe^{-2}$

Figures 11 to 13 depict the mean concentration θ_m with time for different values of Hartmann number, reaction rate parameter and porous parameter. Figure 11 and 12 shows that decrease in θ_m with increasing the value of Hartmann number and reaction rate parameter. This phenomenon occurs due to the enhanced Lorentz force, which reduces the flow velocity and increases the residence time of the solute, leading to increased reaction and reduced mean concentration. Figure 13 show the plots of time dependent mean concentration versus for different values of porous parameter. It is observed that the mean concentration increases with increasing porous parameter, but it is reverse while increasing time. Figures 14 to 16 depict the mean concentration θ_m with X for different values of Hartmann number, rheological parameter and porous parameter.

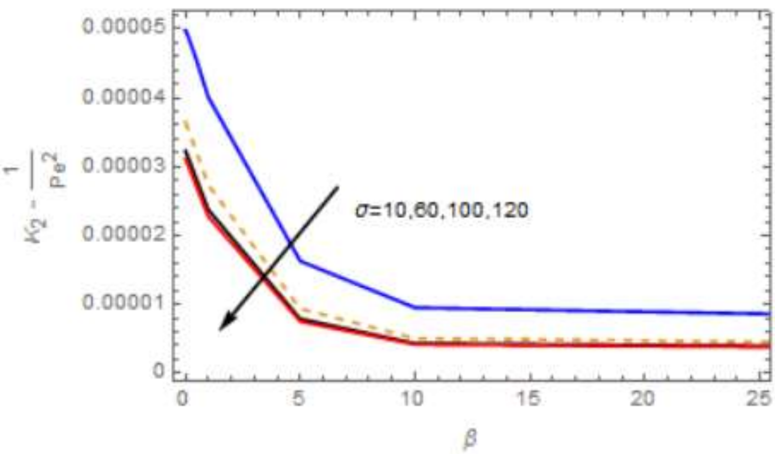

Figure 9: Impact of σ on $K_2(\tau) - Pe^{-2}$

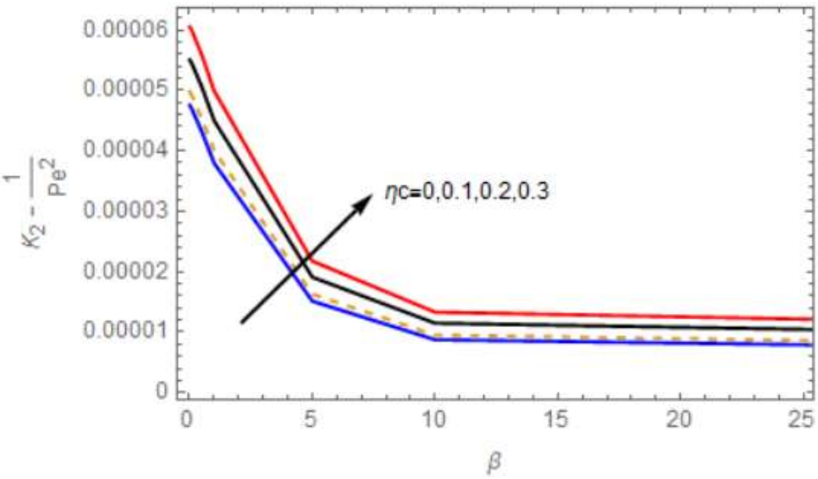

Figure 10: Impact of η_c on $K_2(\tau) - Pe^{-2}$

Figure 14 shows that increase in peak of θ_m with increasing the value of Hartmann number. This can lead to a more uniform distribution of solutes, resulting in a higher peak mean concentration. From Figure 15 it is evident that decrease in θ_m with increasing the value of rheological parameter. When the breadth of the channel or rheological parameters (like viscosity) increase, the peak of mean concentration in blood flow decreases. A wider channel allows for more dispersion of the solute, leading to a more uniform distribution and a lower peak concentration. Similarly, increased viscosity slows blood flow and reduces mixing, causing the solute to spread more evenly, which also results in a decrease in the peak concentration.Figure 16 show the plots of time dependent mean concentration versus X for different values of porous parameter. It is observed that the mean concentration decreases with increasing porous parameter but it reverse after reaching peak of mean concentration.

The aforementioned conclusions make it easier to understand a number of physiological processes, such as the transport of nutrients and drugs through the human circulatory system. Blood oxygenators and other artificial blood equipment may additionally be utilised this. Blood flow in the human circulatory system is known to be influenced by elements such as the branching and curvature pulsatile flow, the elastic characteristics of the arterial wall, and other factors. Besides the effects of these problems, the non-Newtonian nature of blood is a crucial factor in the movement of any passive species in the blood stream (Ramana and Sarojamma, 2012).

5.Conclusion

The dispersion coefficient drops when the wall catalyses the reaction. It is possible to draw some general mathematical conclusions from this study in addition to the biomechanical applications mentioned. The solute dispersion in a non-Newtonian fluid with interphase mass transfer is taken into account in this generalised model, which reduces to that of no wall response as interfacial transport decreases to zero $(\beta = 0)$. In this study, the diffusion coefficient, the classical convective coefficient, and the exchange coefficient which is mostly influenced by the wall response were the three primary dispersion coefficients.

We study the effect of interfacial mass transfer on exchange coefficient, convective coefficient and dispersion coefficient. Wide range of parametric study has been done to understand the underlying physics and draws the following conclusions: Increase in the value of the wall reaction parameter, increases the exchange coefficient but it is unaffected by the remaining parameter such as magnetic field, electric number, rheological parameter, and porous parameter. The effects of couple field, electric number, rheological parameter, and porous parameter with interphase mass transfer must be taken into account in any investigation involving the control of haemolysis.

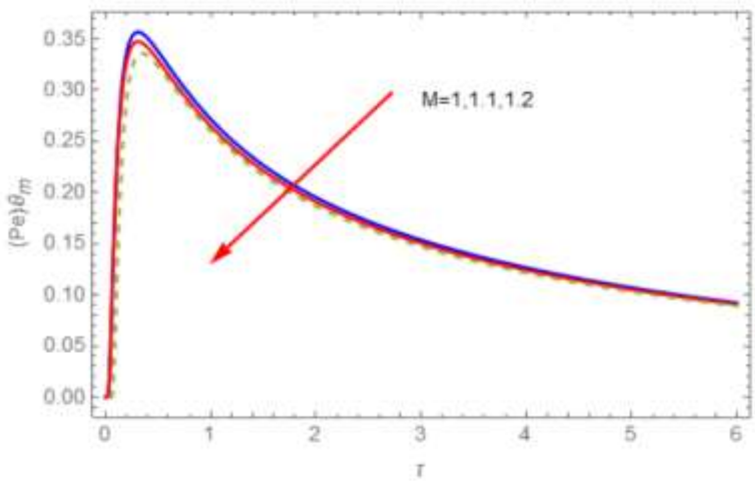

Figure 11: Impact of M on θ_m

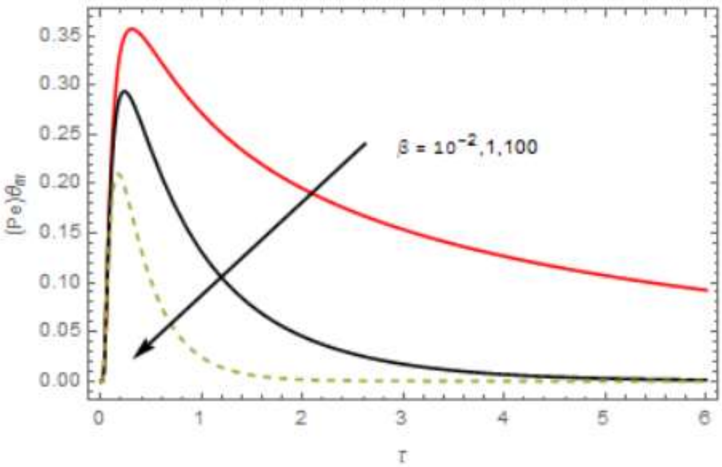

Figure 12: Impact of β on θ_m

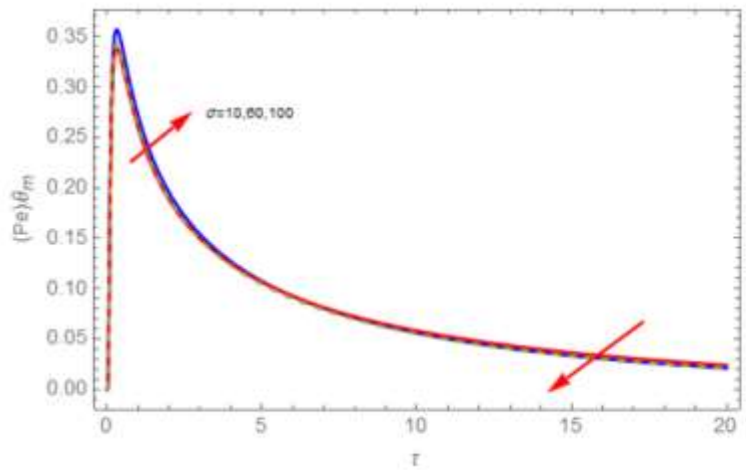

Figure 13: Impact of σ on θ_m

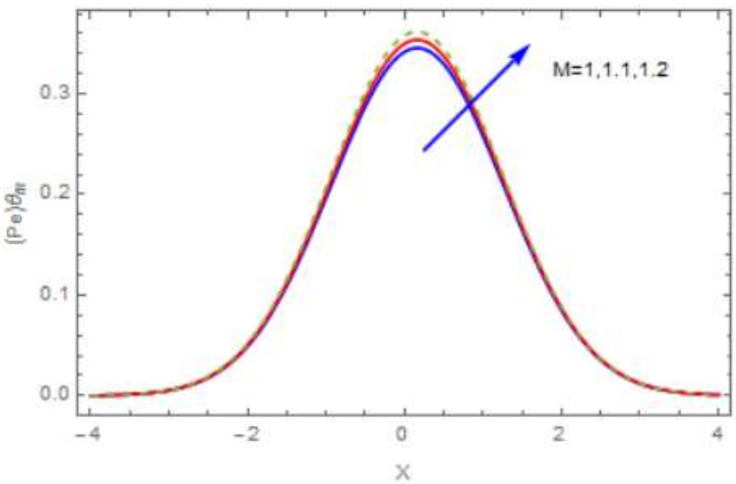

Figure 14: Impact of M on θ_m

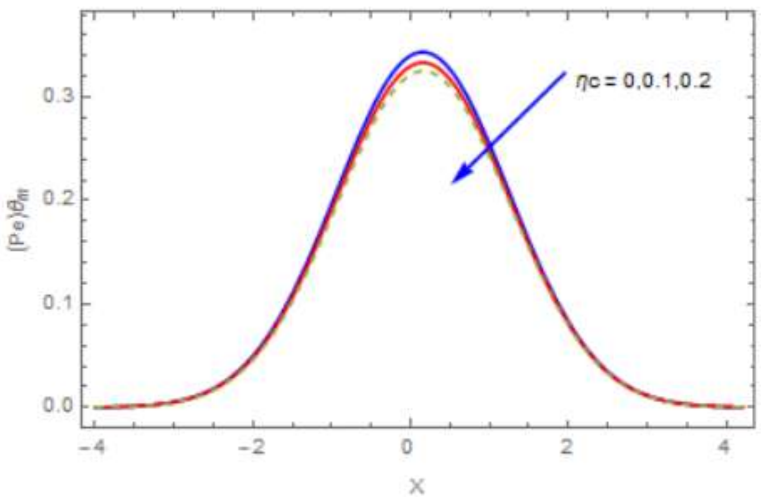

Figure 15: Impact of η_c on θ_m

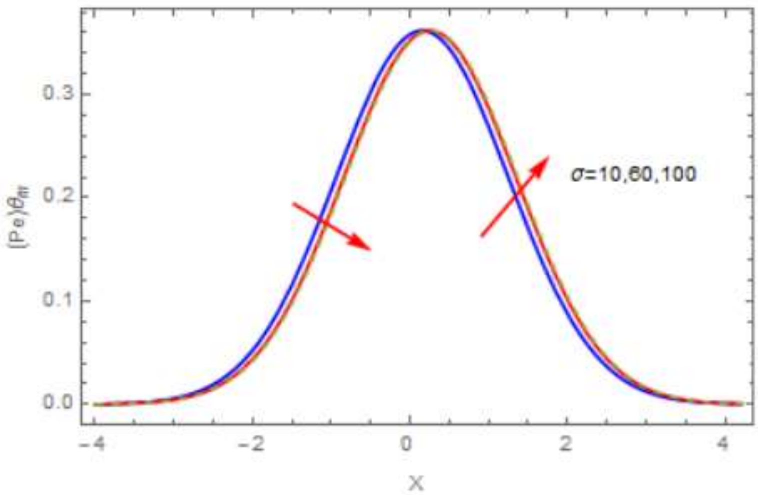

Figure 16: Impact of σ on θ_m

Table 1 Equation roots for $\mu_n \tan \mu_n = \beta$

β	μ_0	μ_1	μ_2	μ_3	μ_4	μ_5	μ_6	μ_7	μ_8	μ_9
10^{-2}	0.099834	3.14477	6.28478	9.42584	12.5672	15.7086	18.8501	21.9916	25.1331	28.2747
0.05	0.22176	3.15743	6.29113	9.43008	12.5703	15.7111	18.8522	21.9934	25.1347	28.2761
10^{-1}	0.311053	3.1731	6.29906	9.43538	12.5743	15.7143	18.8549	21.9957	25.1367	28.2779
0.5	0.653271	3.29231	6.36162	9.47749	12.606	15.7397	18.876	22.0139	25.1526	28.292
1.0	0.860334	3.42562	6.4373	9.52933	12.6453	15.7713	18.9024	22.2126	25.1724	28.3096
5.0	1.31384	4.03357	6.9096	9.89275	12.9352	16.0107	19.1055	22.2126	25.3276	28.4483
10.0	1.42887	4.3058	7.22811	10.2003	13.2142	16.2594	19.327	22.4108	25.5064	28.6106
100.0	1.55525	4.66577	7.77637	10.8871	13.9981	17.1093	20.2208	23.3327	26.445	29.5577

6. APPENDIX

Appendix 1

$$A_1 = \frac{s_5 + s_4 A_2}{s_3}, A_2 = \frac{s_5 s_4 - s_6 s_3}{s_3^2 - s_4^2}, A_3 = 0, A_4 = \frac{-s_7}{6}, A_5 = \frac{A_2 - A_1}{M} CoshM - \frac{We\, s_1 \alpha}{2M^2},$$

$$A_6 = -\frac{(A_2 + A_1)}{M^3} SinhM + \frac{We\, s_1}{6M^2},$$

$$s_1 = \frac{X_0 \alpha_c Pe}{2}, s_2 = \frac{\mathrm{Re}}{Pe} \frac{\partial p}{\partial \xi}, s_3 = (M + \alpha\sigma) e^{M}, s_4 = (M - \alpha\sigma) e^{-M}$$

$$s_5 = \frac{We\, s_1}{M^2} \left(\alpha\sigma(1 - \alpha_c) - \alpha_c \right) + \alpha\sigma U_{p1}, s_6 = \frac{We\, s_1}{M^2} \left(-\alpha\sigma(1 + \alpha_c) - \alpha_c \right) - \alpha\sigma U_{p2},$$

$$U_{p1} = -\frac{1}{\sigma^2 + M^2} \left(\frac{\mathrm{Re}}{Pe} + We\, s_1 (1 - \alpha_c) \right), U_{p2} = -\frac{1}{\sigma^2 + M^2} \left(\frac{\mathrm{Re}}{Pe} + We\, s_1 (1 + \alpha_c) \right)$$

REFERENCES

Annapurna, N. and Gupta A. S.,(1979).Exact analysis of unsteady m.h.d. convective diffusion Proc.R.Soc.Lond.A. 367, 281-289.https://doi.org/10.1098/rspa.1979.0088.

Beavers G.S. and Joseph D.D., 1967.Boundary conditions at a naturally permeable wall. J.Fluid Mech., Vol.30, 197-207.

Cooney D.O., (1976), Biomedical Engineering Principles: An Introduction to Fluids, Heat and Mass transport Processes, First edition, Marcell Dekker, New York.

Gill W.N., and Sankarasubramanian R., 1970. Exact analysis of unsteady convective diffusion, Proc. Roy. Soc. London, A 316, 341-350.

Indira, R., M. Venkatachalappa and P. G. Siddeshwar (1996). Effect of wall permeability and tissue fluid flow on the unsteady convective diffusion of solute in a couple stress fluid flow. Modelling Measurement and Control, France 53(2), 31-39.

Jayaraman G., Lautier A., Bui-Mong Hung, Jarry G. and Laurent D., (1981), Numerical scheme for modelling oxygen transfer in tubular oxygenators, Medical & Biological Engineering & Computing,19, 524-534.

Lightfoot E.N., (1974), Transport phenomena in living system, JohnWiley and Sons, New York.

Manjula, G. J. (2008). Mathematical Modelling of some complex fluids in composite layers, Ph.D. thesis, Bangalore University, India 90-112.

Middleman S., (1972), Transport phenomena in the cardiovascular system, Sixth edition iley Interscience, Chapter 3, 118.

Misra J.C., and Adhikary S.D.,2017, Flow of a Bingham fluid in a porous bed under the action of a magnetic field: Application to magneto-hemorheology, Engineering Science and Technology, an International Journal, 20, 973–981.http://dx.doi.org/10.1016/j.jestch.2016.11.008.

Nirmala P. Ratchagar and Vijaya Kumar, (2015).Exact analysis of Unsteady Convective Diffusion for Blood Flow with Interphase Mass Transfer In Magnetic Field,Bangmod Int. J. Math. & Comp. Sci.1(1), 63- 81.http://Bangmod-Jmcs.Kmutt.Ac.Th/

Ramana B. and Sarojamma G., (2012), Unsteady convective diffusion in a Herschel-Bulkley fluid in a conduit with interphase mass transfer, International Journal of Mathematical Modelling and Computations, 2(3), 159-179.

Rudraiah.N., Mallika K.S and Sujatha N.(2016). Electrohydrodynamic Dispersion with Interphase Mass Transfer in a Poorly Conducting Couple Stress Fluid Bounded by Porous Layers, Journal of Applied Fluid Mechanics, Vol. 9, No. 1, 71-81.

Sankara R.,(1995), Introduction to Partial Differential Equations, Third edition, Prentice Hall of India.

Sakarasubramanian, R. and Gill, W.N.(1973). Unsteady convective diffusion with interphase mass transfer. Proc. Roy. Soc. London, A 333, 115-132.

Siddheshwar, P.G., S. Manjunath and Sripad (2000). Effect of interphase mass transfer on unsteady convective diffusion: Part I, Plane-Poiseuille flow of a power law fluid in a channel. Chemical Engineering Communications. 180(1):187-207.DOI:10.1080/00986440008912208

Singh, J., & Kumar, V. (2020). Numerical study of electric field effects on synovial fluid dynamics. Journal of Biomechanics, 98, 109433.

Siti Nurul Aifa Mohd Zainul Abidin, Nurul Aini Jaafar and Zuhaila Ismail.(2024), Mathematical analysis of unsteady solute dispersion in Herschel-Bulkley fluid with interphase mass transfer, AIP Conf. Proc. 3128, 020002.https://doi.org/10.1063/5.0215017

Tripathi, D., & Kumar, V. (2020). Electrokinetic effects on blood flow through a narrow channel. Journal of Fluids Engineering, 142(10), 101202.

Taylor G.I., (1953), Dispersion of soluble matter in solvent flowing slowly through a tube, Proceedings of the Royal Society of London A., 219(1137), 186-203.

Taylor G.I.,(1954), Conditions under which dispersion of a solute in a stream of solvent can be used to measure molecular diffusion, Proceedings of the royal society A, 225, 473-477.